Bending of apricot tree branches under the weight of axillary growth: test of a mechanical model with experimental data

Tancrède Alméras, Joseph Gril, Evelyne E. Costes

Trees (2002) 16:5–15
DOI 10.1007/s00468-001-0139-1

ORIGINAL ARTICLE

Tancrède Alméras · Joseph Gril · Evelyne Costes

Bending of apricot tree branches under the weight of axillary growth: test of a mechanical model with experimental data

Received: 19 February 2001 / Accepted: 19 October 2001 / Published online: 29 November 2001

Abstract Stem orientation is an important factor for fruit tree growth and branching habit since it influences fruit production as well as training practices. A mechanical model of the bending of a stem under axillary load was written and evaluated using experimental data on apricot trees (*Prunus armeniaca* L.). A set of 15 1-year-old stems of various shapes was observed during the early stage of the growing season when radial growth is still negligible and the loading of the stem increases considerably. The structural modulus of elasticity (MOE) of the stems was estimated through in situ bending tests assuming homogeneous material behaviour. The effect of viscoelasticity was observed through creep tests performed on similar stems during winter. Inputs of the model are initial shape, initial diameter, and final load, defined at various positions along the stem. The final shape was simulated based on different mechanical assumptions, and compared to observations. Assuming small deflections resulted in an underestimate of the mean slope variation of 48%, accounting for large displacements reduced this underestimate to 29% and accounting for viscoelasticity reduced it further to 14%. An adjustment of the structural MOE to fit the final shape led to an excellent fit of the data in most cases, the residual errors for some axes being attributed to material heterogeneity. The use of biomechanical models to predict the shape of fruit trees based on growth parameters, provided adequate assumptions are made, is discussed.

Keywords *Prunus* armeniaca · Biomechanics · Model evaluation · Viscoelasticity · Large deflexions

T. Alméras (✉) · E. Costes
Laboratoire d'Arboriculture Fruitière, ENSA.M-INRA,
2 place Viala, 34060 Montpellier Cedex 1, France
e-mail: almeras@ensam.inra.fr
Tel.: +33-4-99612237, Fax: +33-4-99612616

J. Gril
Laboratoire de Mécanique et Génie Civil, Equipe Bois, CC 081,
Université Montpellier-II, place E. Bataillon,
34095 Montpellier Cedex 5, France

Introduction

Woody species exhibit large architectural diversity. Form and orientation of stems are important components of this diversity and interact with growth and ramification (Smith and Wareing 1964; Wareing and Nasr 1961). In the case of fruit trees, it has been established that stem form and orientation have a qualitative and quantitative impact on production (Lakhoua and Crabbe 1975; Lauri et al. 1997; Lichou et al. 1997), while in a forestry context trunk form is an essential criterion of quality (Kozlowski 1971; Thomas 2000; Timell 1986).

The form of a woody stem is initiated during its elongation by the direction of apex growth (Fisher and Stevenson 1981). This primary direction is modified by the combined effect of three phenomena: bending resulting from the additional self-weight of stems and axillary loads, stem rigidification resulting from radial growth, and secondary reorientation associated with wood maturation (Archer 1986). Fournier and collaborators (Fournier et al. 1991a, 1991b) clarified the application of mechanical principles to the calculation of the deformation of a growing stem. These works underlined the importance of the relative dynamics of stem loading and rigidification, distinguishing "short-term" loading such as wind or snow from "long-term" loading resulting from progressive weight increase of the tree. Qualitative validations of the concepts used in these models have been proposed (Castera and Morlier 1991). A comparison between the mechanical model and experimental data was achieved in the context of the biomechanics of regulation (Fournier et al. 1994); however, this study focused on the regulation of the form of the stem, and did not take into account the actual dynamics of growth. Moreover, most of the work on biomechanical modelling of the form of woody stems has been conducted on forest species, focusing on the change in form and stress distribution of trunks of adult trees. In this context, the time unit is the annual growth ring (Fourcaud and Lac 1996; Fournier et al. 1991a) and the effect of intra-year dynamics of loading and rigidification is disregarded.

The present study is part of a wider project devoted to the genetic selection of apricot trees. One of the goals of this project is to control the form of new varieties. A biomechanical model was thus developed to help understand the relationship between growth characteristics and the form of woody stems, and to simulate the effect of modification of these growth characteristics on stem form.

The aerial architecture of apricot tree has been studied previously in detail by Costes (Costes 1993). Apricot trees present a large diversity of forms which apparently results, at least in part, from the bending of the long branches. The flowering of the apricot tree occurs on 1-year-old stems and blooming precedes vegetative bud break. This is followed by the first stage of fruit growth and development of leafy shoots (Costes et al. 1995; Lichou and Audubert 1989). Radial growth (i.e. the increase in stem thickness) starts later in the season (Costes et al. 2000). During the period preceding radial growth, the 1-year-old stems are submitted to large load increments. This period attracted our interest for several reasons: (1) during this period the intra-year growth dynamic cannot be disregarded, (2) the delay between weight increase and radial growth allows simplified mechanical formulas where the quantity of matter constituting the holding structure can be considered as roughly constant, (3) the large amount of loading implies easily measurable deflections, and (4) bending takes place within a relatively long period allowing one to test the consequences of the viscoelastic behaviour of the stems (Gril and Fournier 1993).

The goal of the present survey is to evaluate, from data measured on 1-year-old apricot tree stems, a mechanical model predicting the amount of bending during a period with no radial growth. The analysis used has much in common with that applied by other authors to the modelling of wind loading of tree trunks (Milne and Blackburn 1989; Morgan and Cannell 1987; West et al. 1989). The present work must be considered as a validation step of the model; both the relevance and the necessity of the mechanical assumptions introduced will be discussed.

Mechanical model of stem bending

Basic model assuming small perturbations

Bending simulation is based on curvilinear beam bending theory with perfect embedment at one end (Timoshenko 1953). The problem is solved in two dimensions: the stem is supposed to remain in a vertical plane. It is divided into n beam elements. The geometry of the ith element (i) in the initial state is described by its diameter (D_i), its length (L_i), and its curvature (C_i^{ini}). All elements are made of the same homogeneous elastic material, characterized by its modulus of elasticity (MOE; E) and density (ρ). The angle between the horizontal direction and the tangent at the point of embedment is given as Φ_0.

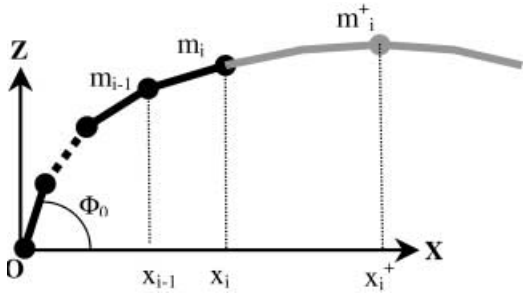

Fig. 1 Data describing the geometry and the load of an axis in a vertical plane. m mass, Φ angle of a segment

In the initial equilibrium, the element i is submitted to the loading due to the self-weight of the stem. Bending results from additional loads defined by their mass (m_i') for each element i. We will neglect the fact that the centres of mass of the axillary products may be significantly distinct from their point of application, and consider that all their mass is concentrated at their base. This approximation will be discussed subsequently.

The deformation of the element i results in a variation of curvature:

$$\Delta C_i = \Delta M_i / EI_i \tag{1}$$

where I_i is the second moment of area of the element (for a circular cross-section, $I=\pi D^4/64$), ΔM_i is the bending moment applied on the element i by the increment of weight of the downward stem portion. Let x_i be the position of the end of the element i in the absolute coordinate system (O, X, Z), x_i^+ and m_i^+ the position and mass, respectively, of the centre of mass of the downward stem portion (Fig. 1). The total mass of the element i, including the self-weight and the loading, is:

$$m_i = m_i' + \pi \rho L_i D_i^2 / 4 \tag{2}$$

The bending moment applied to the element i is:

$$M_i = \left(x_i^+ - x_i\right) g\, m_i^+ \tag{3}$$

where g is the gravity constant. The mass of the downward stem portion from i–1 is:

$$m_{i-1}^+ = m_i^+ + m_i \tag{4}$$

The position of its centre of mass is:

$$x_{i-1}^+ = (m_i^+ x_i^+ + m_i x_i)/m_{i-1}^+ \tag{5}$$

The recurrent application of these formulas along the stem axis, from the apex toward the insertion, allows one to calculate the bending moment applied to each segment in a given geometrical configuration (Blaise et al. 1992).

However, the deformation derived from Eq. 1 corresponds to an equilibrium solution only if the moment (ΔM) is calculated in the final configuration. In the case where the small deflection assumption (SDA) is valid, the change in bending moment induced by the deformation can be neglected such that the moment calculated in the final configuration can be approximated by that calculated in the initial configuration (Fig. 2). The deformed configuration of every element can then be given by the new curvature:

$$C_i = C_i^{\text{ini}} + \Delta M_i / EI_i \tag{6}$$

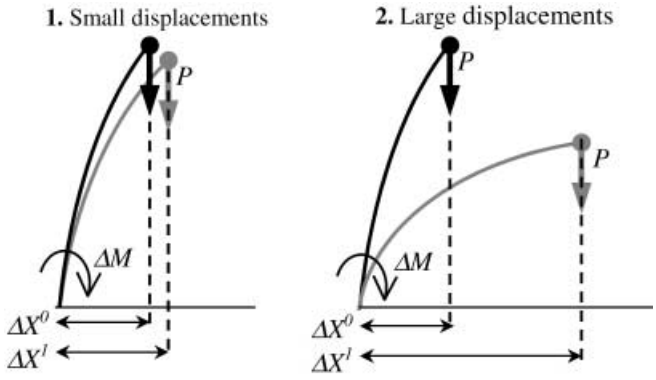

Fig. 2 Calculation of the bending moment: assuming small displacements ($\Delta M=\Delta X^1P\approx\Delta X^0P$) (*1*); considering large displacements ($\Delta M=\Delta X^1P\neq\Delta X^0P$) (*2*)

The length (assumed unchanged) and new curvature of all elements allow one to rebuild the whole form of the stem. If Φ_i is the angle of the segment *i*, the angle of the segment *i+1* becomes:

$$\Phi_{i+1} = \Phi_i + C_i L_i \tag{7}$$

The position of its extremity is given by:

$$x_{i+1} = x_i + L_i \cos(\Phi_{i+1}) \tag{8}$$

$$z_{i+1} = z_i + L_i \sin(\Phi_{i+1}) \tag{9}$$

The position of all segments of the stem can be calculated by the recurrent application of these formulas from the stem insertion toward the apex.

Accounting for large displacements

In the case of large displacements, the deformation calculated with the SDA is not a valid approximation of the solution. Indeed, since the bending moments depend on the lever arm of the loads, they vary strongly during deformation (Fig. 2), and the solution is no longer compatible with the requirements of static equilibrium. To take this phenomenon into account, bending moments must be recalculated in the deformed configuration, and a new stem form derived again from the deformations associated with the new moments. The operation is repeated until the difference in form is lower than a given threshold. In other words, a correct solution verifying both conditions of static equilibrium and kinematic relations has been reached as soon as it remains practically unchanged by a cycle of recalculation of bending moments (from apex to insertion) followed by form reconstruction (from insertion to apex). This iterative resolution of the problem can be subjected to problems of convergence, solved by the introduction of a damping factor (Craig 1989).

The method of Morgan and Cannell (1987), based on the use of a transport matrix, differs from ours by the ordering of operations, as they recalculate the moments together with reconstruction of the shape. As soon as a stable form has been reached both methods should lead to the same solution. West et al. (West et al. 1989) have proposed an alternative approach with an integro-differential equation technique based on the same physical principle, but they did not apply it to conditions requiring the consideration of large displacements. None of these models accounted for an initial geometry differing from a straight line, as is allowed in the present formula.

The calculations were easily performed with the help of spreadsheets of Microsoft Excel97 associated with Microsoft Visual Basic commands. The stem structure is composed of 50 elements. Large displacement calculations have been validated by comparison with well-known analytical solutions of elastic buckling (Timoshenko 1966).

A procedure of structural MOE adjustment has been integrated into the model. It determines the value of MOE minimising the distance between the simulated final configuration and a target configuration. The distance used is the sum of squares of distances between the points of the stem (least square criterion).

Accounting for viscoelasticity

Woody material shows viscoelastic behaviour (Koll-Mann and Côté 1968). As a result, the deformations induced by a given load vary with time. To take this phenomenon into account, it is necessary to know the temporal evolution of the material properties, characterized here by a time-dependent MOE [$E(t)$]. The deformation at time t_1 of an element submitted to the bending moment ΔM since time t_0 becomes:

$$\Delta C(t_1) = \Delta M / E(t_1 - t_0) I \tag{10}$$

The deformation at time t_1 is equivalent to the instantaneous deformation of an elastic material whose MOE is $E(t_1–t_0)$.

Since time is not an explicit parameter in our model, viscoelasticity is taken into account through the use of an equivalent structural MOE at the final date. The calculation of this modulus considers the dynamics of the loading as well as the $E(t)$ law, and is based on the principle of superposition (Lemaitre and Chaboche 1985). Let a beam element be submitted at successive dates (t_1, t_2,..., t_k,..., t_f) to permanent loads characterized by their bending moments (ΔM_1, ΔM_2,..., ΔM_k,..., ΔM_f). At time t_f, the curvature increase caused by the load added at time t_k is:

$$\Delta C_k(t_f) = \Delta M_k / E(t_f - t_k) I \tag{11}$$

The increment of curvature caused by the cumulation of all loads is:

$$\Delta C(t_f) = \sum [\, \Delta C_k(t_f) \,] = \sum [\, \Delta M_k / E(t_f - t_k) I \,] \tag{12}$$

The equivalent MOE at time t_f is:

$$E^{ve} = \Delta M / I \Delta C(t_f) \tag{13}$$

where $\Delta M=\Sigma(\Delta M_k)$ is the total bending moment imposed on the element.

The equivalent MOE finally becomes:

$$E^{ve} = \Delta M / \sum [\, \Delta M_k / E(t_f - t_k) \,] \tag{14}$$

Materials and methods

Material

In order to check the model based on a large range of morphology, three varieties of apricot tree (*Prunus armeniaca*) with contrasting stem forms have been chosen for the survey (Fig. 3). Lambertin no. 1 has an upright form, Modesto a spreading form, and Palsteyn a weeping form (Lichou and Audubert 1989). The trees were planted in 1993 in the experimental orchard of the Fruit Arboriculture Laboratory of INRA (Montpellier, France). The trees had been grafted on seedlings of Manicot rootstock. The studied material is from six Lambertin trees trained in a Y form, eight Modesto trees trained in a Y form and four Palsteyn trees trained in a goblet form with four limbs. During the winter 1997/1998, the trees were pruned to induce the development of long shoots.

In the beginning of 1999, five 1-year-old stems of each variety were selected for the dynamic description of growth and bending. All were made of a single growth unit, 70–170 cm long, and carried no sylleptic branches. The stems were observed during 1999, which corresponded to their first year of fruit production and ramification. The ramification process leads to the development of axillary leafy shoots. Two types of shoots are usually distinguished. Short shoots originate from organs entirely pre-formed in the bud; their length does not exceed a few centimetres. Long shoots contain longer internodes and they continue elongating after bud break. Since apricot trees exhibit a sympodial ramification, stem extension requires the elongation of the bud located below the dead apex. This bud is equivalent to any lateral bud of the stem; therefore, in our survey, extension growth is not distinguished from other axillary shoots. The presented results are restricted to the period between the flowering of the most precocious variety (week 7 of the year) and fruit maturity of the most precocious variety (week 22 of the year).

During 1999, 20 additional stems and 150 fruits of each variety were used to establish relations between the morphology of the axillary productions and their mass. The chosen stems were similar to the samples used for growth observation. During winter 1999/2000, three other stems of each variety, similar to those of the main sample, were used for the creep tests.

Record of loading history

The axillary productions associated with each node were observed repeatedly during the survey: at bloom, 5–6 weeks after bloom, then every 2–3 weeks until fruit maturity. Three types of axillary production were distinguished: fruits, short shoots and long shoots. The diameter of the biggest transverse dimension of the fruits was measured. As most of the mass of the short shoots is made of the leaves, only the number of leaves was recorded. For the long shoots, the number of leaves, the base diameter and length of the shoot were recorded.

Since the stems were observed during the whole season, it was not possible to measure the mass of the organs directly. For each type of production and for each variety, allometric relations were established to estimate the mass of the organs from the measured data. All axillary products of the stems used for this purpose were observed in the same way as those of the survey, then weighed with a precision of ±0.1 g. In a similar way, 30 fruits of each variety were measured and weighed at five stages to establish the relation between the diameter and the mass of the organs. The relations between leaf number and mass of short shoots, between diameter and mass of fruits and between length, base diameter and mass of long shoots, were then established.

Record of diameter growth history

Just before flowering, the stems were marked at 5-cm intervals with a Typex ring to ensure fixed measurement points throughout the study. At each point, stem diameter was measured with electronic callipers. These data were recorded on the same dates as the measurements on axillary products. Considering the main role of the diameter data for the mechanical simulation, two precautions were taken: (1) we checked the circularity of the stem section by measuring the diameter in two perpendicular directions, (2) during the survey, the diameter was measured perpendicularly to the stem axis, with the direction of the handle in the vertical plane of stem bending.

To characterize the radial growth of every stem globally, the mean diameter (D_m) was defined as the average of the diameters recorded at all measurement points. The second moment of area corresponding to the mean diameter ($I_m=\pi D_m 4/64$) was used to compare stems from a mechanical point of view (Alméras 2001).

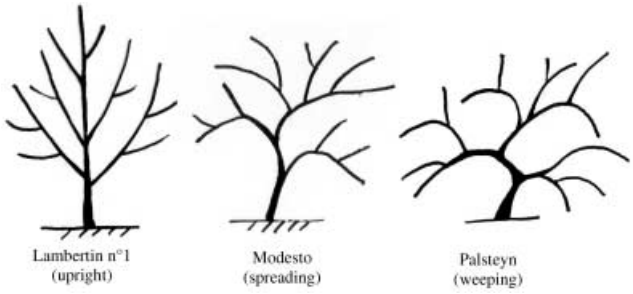

Fig. 3 Three apricot tree varieties with contrasting forms

Record of bending history

The position of each measurement point was recorded using a magnetic three-dimensional (3D) Polhemus digitizer (Polhemus 1993) and data acquisition software (Adam et al. 2000). These measurements were done 1–2 weeks after flowering, then every 3–4 weeks until fruit maturity.

Various operations were performed for each scatter describing a given stem.

1. To ascertain the reliability of the data, the points were visualized and the real length of segments was compared to that derived from coordinates.
2. In view of the simplified in-plane mechanical calculations, the points were projected in their vertical plane (Fig. 4), using classic data-reduction methods (Seber 1984). The stems were well represented in this plane, since the average distance between initial and projected points was <1% of the length of the stems.
3. Coordinates were finally expressed in a 2D coordinate system where the origin is the insertion point of the stem, and the *x*-axis is the direction of the scatter (Fig. 4).

To characterize the intensity of bending, some authors use the variation of the tip coordinate (Leiser and Kemper 1973; Milne and Blackburn 1989; Morgan and Cannell 1987). However, this criterion gives much weight to local effects around the tip. In this study, the orientation of a stem axis was quantified as the mean slope (i.e. the average slope of the segments), and the bending between two dates was characterized by the reduction of the mean slope, designated “leaning”.

Interpolation of the data

For practical reasons, like differences between varieties’ phenology or climatic constraints associated with in-field digitalization, the various data could not be recorded simultaneously. To homogenise the data format, measured values were sometimes complemented by weekly values interpolated linearly between the dates of nearest measurement.

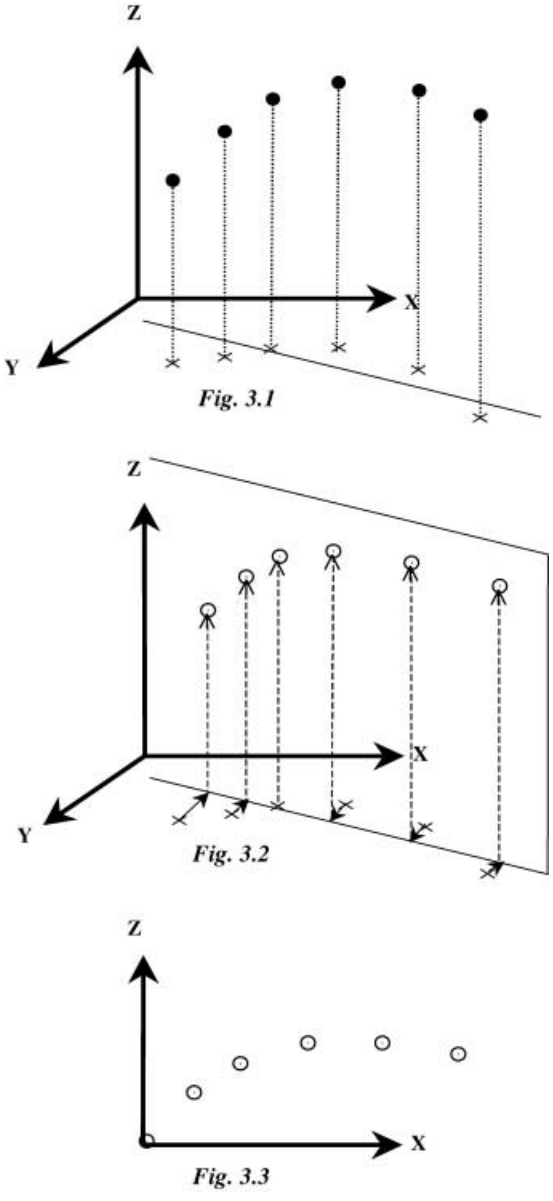

Fig. 4 Adapting geometrical data: determination of the projection plane (*1*); projection of the points (*2*); Two-dimensional representation after translation and rotation (*3*)

The geometric measurements were achieved every 5 cm along the stems whereas the bending model requires 50 elements of discretization. Consequently, the steps of discretization differed from those of model input; these were obtained by linear interpolation between the nearest points.

In situ elastic bending test

The structural MOE of the stems was estimated in situ by a bending test. The initial form of the stem was digitized, then a known weight was attached at a given position of the stem, and the form was digitized again about 10 min later. The stem diameter was measured at various positions along the stem axis. This test was performed for every stem of the sample just before flowering with a weight of 185 g attached at the point three-quarters of the way along the total stem length.

A procedure of assessment of structural MOE was used to obtain a unique value of MOE, assuming that the stem is composed of homogeneous material. The value was determined through the use of the mechanical model, thus ensuring a correct accounting of large displacements.

In situ creep bending test

During winter 1999–2000, an in situ creep test was conducted on three stems of each variety to evaluate the viscoelastic behaviour of the stems. The test was done in winter so that no growth influenced the loading or the stem rigidity. The test was similar to that of instantaneous bending, except that after 10 min of loading and form recording, the stem was left loaded and the form was digitized 40 min, 3 h, 24 h, 5 days and 32 days after loading. The structural MOE was evaluated at each stage by large-displacement adjustment relative to the initial form before loading. From the values $E(t_1)$..., $E(t_n)$ obtained for the times $t_1...t_n$, a law of time-dependent structural MOE [$E(t)$] can be evaluated.

Results

The results concerning the dynamics of growth and bending, as well as the results of the simulations, have been established for all stems of the sample (five of each variety). They will be presented for the whole sample and illustrated for one typical stem of each variety.

Growth dynamics

In the beginning of the season, the mean diameter of the stems ranged between 5.3 and 8.9 mm and, at week 22, between 5.5 and 12.9 mm. Fig. 5a–c shows the change in I for the three typical stems: clearly, I increases very slowly at the beginning of the season. During the 10 weeks after flowering, I increased by <25% on average for all stems. Afterwards, the rate of growth became faster: I increased on average by 117% between weeks 7 and 22. Table 1 gives I at weeks 7 and 22 for all stems. For comparison, on the same stems, I increased by an average of 600% during the whole year.

Axillary load

The observed stems reached the stage of full bloom by mid February (week 7) for Lambertin and Palsteyn, and by the end of February (week 9) for Modesto. Fertilization of the fruits takes place in the following 2 weeks. The fruits then undergo a first phase of an increase in weight, until the period of pit hardening, about 40 days after flowering (Costes et al. 1995). Vegetative bud break took place for all varieties about 2 weeks after full bloom. On all stems, most nodes produced short shoots carrying three to ten leaves. These shoots opened out their leaves within 2–3 weeks. On the five Modesto and one Palsteyn stem, one or two nodes produced long shoots that continued to grow 4–5 weeks after bud break.

The relations between length and long shoot mass and between diameter and fruit mass were quantified by a

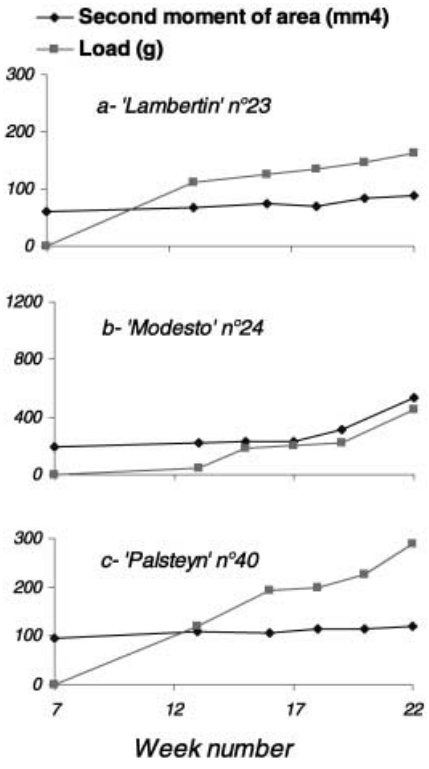

Fig. 5a–c Change in mean second moment of area and axillary load for three axes

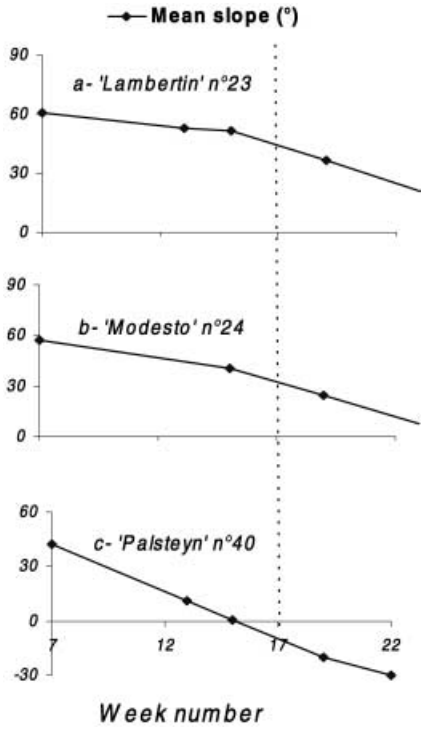

Fig. 6a–c Change in mean slope for three axes

Table 1 Global data for each stem: total axillary load at week 17 (L); mean second moment of area (I) at week 7 (I-7), 17 (I-17) and 22 (I-22), direct estimate of Young's modulus of elasticity (E^0) by in situ bending test, value corrected to take creep into account (E^{ve}), adjusted value (E^{adj}). D Mean distance between points of observed and adjusted configurations

	L (g)	I-7 (mm^4)	I-17 (mm^4)	I-22 (mm^4)	E^0 (MPa)	E^{ve} (MPa)	E^{adj} (MPa)	D (cm)
Lambertin no. 23	130	60	73	89	4,718	3,822	4,301	0.5
Lambertin no. 30	223	314	402	531	3,810	3,086	3,060	1.1
Lambertin no. 32	183	77	79	96	6,552	5,344	2,288	3.3
Lambertin no. 33	101	110	122	160	5,489	4,431	4,001	0.9
Lambertin no. 38	212	183	184	201	6,875	5,589	3,629	0.4
Modesto no. 19	127	86	98	172	5,410	4,792	3,432	1.9
Modesto no. 20	275	266	364	574	6,513	5,770	3,046	2.1
Modesto no. 22	156	190	274	1,052	5,957	5,264	4,289	0.4
Modesto no. 23	133	158	191	464	5,342	4,710	3,642	0.5
Modesto no. 24	202	191	231	531	4,830	4,275	3,198	0.9
Palsteyn no. 30	386	128	165	296	6,582	5,505	8,737	0.9
Palsteyn no. 31	428	158	204	240	4,179	3,527	3,687	0.7
Palsteyn no. 37	163	56	76	91	5,507	4,637	3,139	2.2
Palsteyn no. 39	64	40	46	47	4,285	3,578	3,265	0.5
Palsteyn no. 40	186	95	111	121	4,414	3,706	3,153	2.8

power law ($m=ad^b$), where m is the mass of the organ, d the measured dimension, a and b parameters of estimation. The parameters have been quantified by regression for every variety and every type of organ (data not shown).

For each stem, the total loading was calculated at each date and is shown on Fig. 5a–c for the three typical stems for the period considered. It increased until fruit maturity under the combined effect of shoot and fruit growth. At week 22, the fruit weight represented 50% of the total loading on average, that of short shoots 40%, and that of long shoots 10%.

The mechanical modelling concerned a period between weeks 7 and 17, during which time the radial growth did not exceed 10% of the initial diameter. At week 17, the total load of the stems ranged between 64 and 386 g. Table 1 indicates the mass of axillary loads, as well as the mean I at this date for each stem. One Lambertin and two Modesto trees did not carry any fruit at this date. The other stems carried one to ten fruits. The length of long shoots did not exceed 25 cm at week 17.

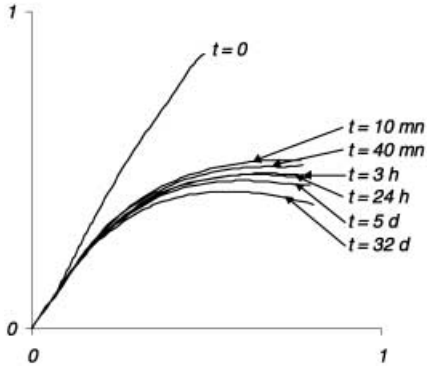

Fig. 7 Change in the shape of a Lambertin axis during a creep test: before bending (t=0), 10 min after bending (t=10 min), 40 min, 3 h, 24 h, 5 days and 32 days after bending

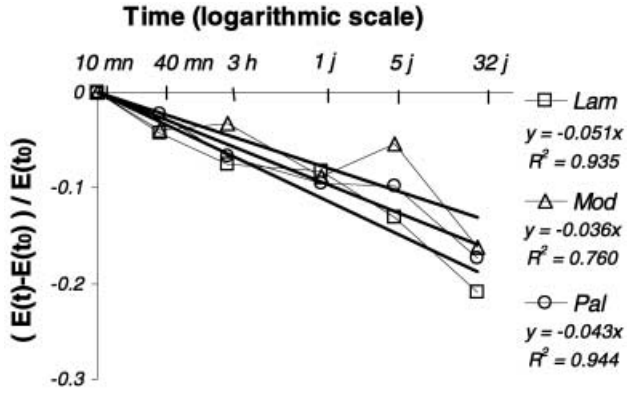

Fig. 8 Relative decrease in the equivalent Young's modulus for the three varieties. *Each point* represents the mean of three stems. Regression lines (passing through 0) and regression coefficients (R^2) for each variety are indicated on the figure

Bending

The mean slope decreased regularly from flowering to fruit maturity, up to a maximal average leaning of 45° (Fig. 6a–c). In the period between weeks 7 and 17, the stems bent by 30° on average. This mean value hides important variations among stems: leaning at this date ranged between 7° and 58°.

Mechanical properties of the stems

The structural MOE of every stem (E^0) has been determined by adjustment from the data of instantaneous loading (Table 1).

The creep tests confirmed the existence of viscoelastic behaviour. The bending of stems submitted to a constant load increased with time (Fig. 7). This corresponds to an apparent MOE decreasing with time (Fig. 8). For each variety and at each date of measurement, the curves give the average for all three stems of the relative reduction in MOE, given by the ratio:

$$[E(t_0) - E(t)]/E(t_0) \quad (15)$$

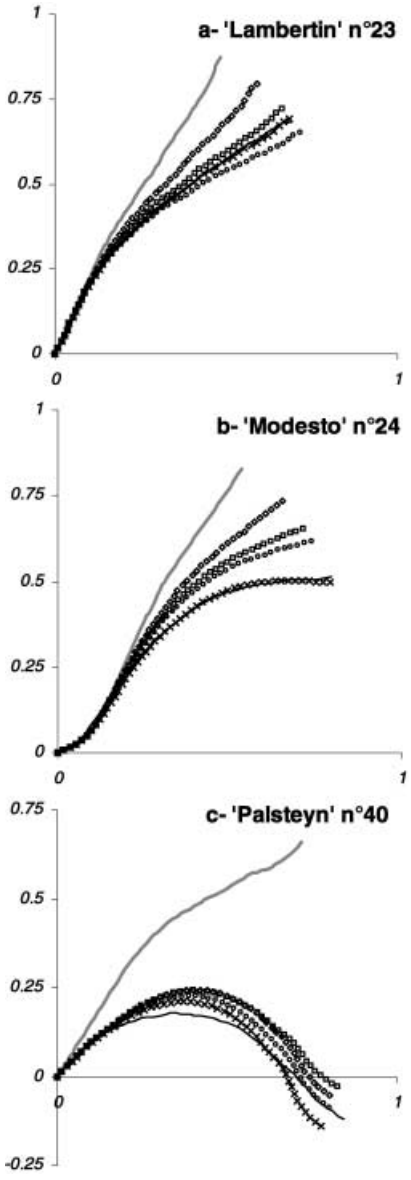

Fig. 9a–c Observed initial (—) and final (—) form of three axes, and simulated final form under different assumptions: small displacements and structural modulus of elasticity (E^0) (◇), large displacements and E^0 (□), large displacements and equivalent E (○), large displacements and adjusted E (×)

where $E(t_0)$ is the structural MOE after 10 min of loading. The curves were approximated by a linear regression as follows:

$$E(t) = E(t_0)[1 - \alpha \log(t/t_0)] \quad (16)$$

The slope (α) characterizes the degree of viscoelasticity of the material. The values of α and the coefficients of determination are indicated in Fig. 8.

These relations allow one to calculate, for each stem, $E(t)$, with $E(t_0)$ taken as the instantaneous MOE (E^0) of the given stem. The equivalent modulus at week 17 (E^{ve}) can be calculated using Eq. 14, for each stem, by taking into account the loading history (Table 1).

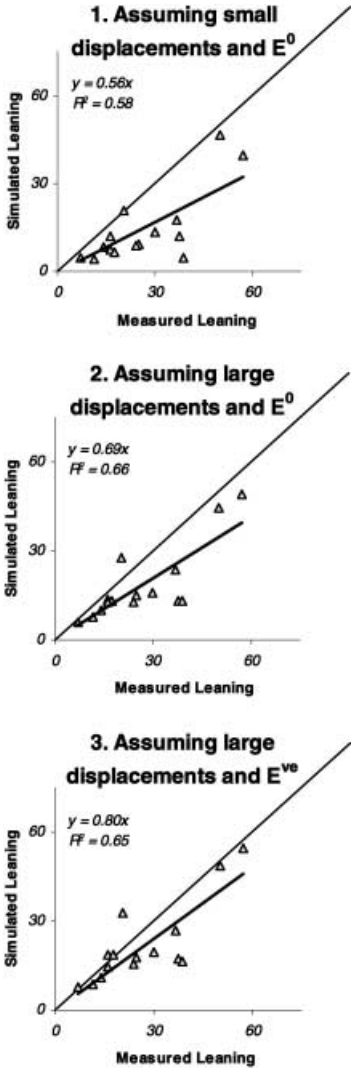

Fig. 10 Comparison between measured and observed leaning for all axes, with different sets of assumptions

Making use of the mechanical model

For each stem, we calculated the bending predicted by the mechanical model. The possible variation of the angle of embedment, resulting from movements of the holding branch, was taken into account. To carry out the calculation, the model requires:

1. Global stem data: inclination of stem base before and after bending, total stem length, material MOE and density.
2. For each 50 elements: curvature and diameter in the initial state, and attached load.

For each stem, initial state data (base angle, total length, curvature, diameter) have been specified from the measurements of week 7, and final state data (base angle and loading) from those of week 17. Measured geometrical data at week 17 were used to evaluate the quality of the model. The calculations of deformation were achieved using three sets of assumptions:

1. Small displacements (SDA) and structural MOE (E^0).
2. Large displacements and structural MOE (E^0).
3. Large displacements and structural MOE (E^{ve}) taking into account the viscoelasticity.

Fig. 9a–c shows the results of the simulations for the three typical stems. To facilitate the comparison between stems of different length, the graphs were normalized by the total length of the stem. Fig. 10 compares, for all stems, their simulated and observed leaning.

Discussion

Evaluation criteria of the models

We distinguished between three levels to evaluate the models:

1. The global level, which involves the whole sample. The errors detected at this level reveal a global insufficiency of the model, that depends little of the individual features of the stems. They can be assessed by comparing the average values of simulated and observed leaning, or, in a practically equivalent way, by comparing the slopes of the regression line obtained from these values to 1 (Fig. 10).
2. The individual level concerns the simulation of each stem. The errors at this level result from specific features of individual stems. They generate a bigger dispersion in the diagrams comparing the simulated and observed leaning, resulting in a lower coefficient of determination.
3. The local level concerns the different parts of a given stem. The errors made at this level cannot be revealed by the comparison of simulated and observed leaning, which are, by definition, averaged over the whole stem. The global simulation of a given stem might well be of good quality, without the simulated form corresponding locally to the observed form. These effects can only be observed by comparing locally the simulated and observed forms, provided they are not masked by individual and global errors.

Inadequacy of SDA and necessity to account for large displacements

The comparison between the simulation made with and without SDA (Fig. 10) shows clearly the unsuitability of this assumption in the case of young fruit tree stems. Leaning is globally underestimated by 48% on average when assuming SDA. This underestimate is reduced to 29% by accounting for large displacements.

The effect of the SDA is, however, more complex than a systematic underestimate as can be seen in Fig. 9. In Fig. 9c, leaning calculated with the simplifying assumption (SDA) is superior to that calculated without. The effect of SDA actually depends not only on the magnitude of the deformation, but also on the initial stem

orientation. The more vertical the stem, the greater the error. As a result, SDA not only leads to a global error on the mean of the simulated leaning, but also to a higher dispersion of individual errors. This effect results in a lower coefficient of determination between observed and simulated leaning (R^2=0.58 with SDA vs. R^2=0.66 when accounting for large displacements).

Previous authors discussing the limits of validity of SDA usually disregard the influence of stem orientation. For instance, Milne and Blackburn (Milne and Blackburn 1989) consider that the endpoint deflection calculated under SDA should be <25% of the stem length to ensure the applicability of SDA. This is only true, however, with respect to a load acting transversely to the stem direction, as was the case in their work. The more axial the load, the less applicable becomes such a criterion. At the opposite extreme, when the load is close to axial and buckling occurs, the use of a large displacement formulation cannot be avoided although a SDA calculation would predict a negligible deflection.

Improvement through accounting for viscoelasticity

In the model, viscoelasticity has been taken into account indirectly through the calculation of an equivalent MOE at the final date. It results in an average MOE decrease of 15%. Leaning simulated with this corrected value remains underestimated on average in relation to the observed leaning, but by only 14%. Compared to the underestimate of 29% obtained with the instantaneous structural MOE, this is a substantial improvement. The method used here considers the viscoelasticity of all stems of a variety globally, and does not permit one to detect differences of behaviour between individuals. This explains why the coefficient of determination is not improved by this correction.

We note that this calculation disregards the viscoelastic effects associated with the variations of bending moment during the period of measurement. Only a calculation involving time explicitly, with a recalculation at every step of the bending moments in the deformed configuration, would permit one to take into account these second-order effects.

Possible origin of global and individual errors

The difference between the measured stem form and that simulated by the model, after accounting for large displacements and viscoelasticity, can be attributed to various causes, including the quality of the input data as much as that of the model itself.

First of all, the assessment of stem loading can be discussed. Loading was estimated indirectly through allometric laws established on a relevant sample. The final uncertainty on the load is about 10%, but the estimates should not be biased as they have been established on a relevant sample. Therefore, this factor can explain individual gaps but cannot be responsible for the globally underestimated leaning. On the other hand, the loading imposed by axillary shoots was assumed to be concentrated, thus neglecting the lever arm of long shoots and, automatically, underestimating the leaning of individuals with such shoots. However, these shoots represent a small part of the load and their length did not exceed 25 cm. Calculations made separately show that they can only account for a small part of the observed errors.

Furthermore, the assumption of no radial growth during the period is questionable since it was not strictly zero: the diameter increased by 1–10% of the initial diameter. The newly formed tissues have potentially three effects (Fournier et al. 1991a): (1) they act like an additional load; (2) once lignified, they participate in the support of the stem; (3) the maturation strains occurring during their lignification induces a slight correction of the stem orientation. Effect (1) works in accordance with the observed error, (2) and (3) opposite to it. The consequences of these factors are not included in the present model and have not been quantified.

Evidencing local errors by fitting the structural MOE

Local errors produced by the model could not be checked unless individual errors were eliminated. This was obtained by adjusting the structural MOE. For every stem, the value of MOE minimising the distance between the simulated and the measured configuration was calculated. Table 1 gives the adjusted structural MOE for each stem, as well as the average distance between the points of the simulated and measured configuration. Fig. 9a–c shows the results of the simulations based on the adjusted structural MOE for the three stem types. In eight cases out of 15, the average distance is <1 cm and the simulated configuration is almost identical to the measured configuration. The quality of the simulations with only one adjusted parameter shows that the model accounts for most of the locally involved phenomena. However, in five cases, the difference was rather high (see Fig. 9c, for example). The poor quality of the adjustment can be assigned to local effects not taken into account by the model, since the structural MOE adjustment has corrected the individual effect on the whole stem.

The method used to determine MOE is similar in principle to that used, for instance, by Leiser and Kemper (Leiser and Kemper 1973) or Morgan and Cannell (Morgan and Cannell 1987), except that these authors fitted the deflection of the loaded point, whereas our criterion involved all measured positions along the stem axis. Another specific point of our work is that it concerns loading in natural conditions, i.e. the load increase during the growing season; our previous predictions of stem geometry were based on the value of structural MOE measured before the start of the growing season.

Errors observed at the local level after fitting MOE can be attributed to material properties. The material of

stems was assumed to have homogeneous elastic properties. Measurements of MOE of beam portions taken at different positions along the stems (unpublished data) did not show any significant correlation between the MOE and the position in the annual shoot, thus justifying the use of a structural value. However, a longitudinal variation of the MOE is likely to occur in some stems. In Fig. 9c, for example, a decrease in the MOE along the stem could explain the poor quality of the simulation based on structural MOE adjustment, with bending being underestimated in the basal part of the stem, and overestimated in its terminal part.

The model could be improved by accounting for longitudinal variations in MOE. Experimental data on these variations can be obtained in a non-destructive way, through the same type of in situ bending test used here. Moulia (1993) used this type of test on corn leaves with a local analysis that consists of calculating, for any abscissa (s) of the stem, a local MOE [$E(s)$]. The MOE is given directly by $E(s)=\Delta M(s)/I(s)\ \Delta C(s)$, where $\Delta M(s)$ is the variation of bending moment due to the external load at s, and $\Delta C(s)$ the variation of curvature at s. This method requires the calculation of curvature variations, which involve the second-order derivatives of the measured coordinates. Therefore, it is very sensitive to small measurement errors; to achieve a good degree of precision a large number of points must be digitized.

Implications for the modelling of tree development

In the case of young fruit tree stems, variations of bending moment during deformation (i.e. large displacements) and viscoelastic behaviour of the stem must be taken into account to achieve a good agreement between simulations and observations. For older stems, load increments act on a thicker, more rigid structure, yielding much smaller displacements. Therefore, the error resulting from the SDA is likely to be smaller in aged structures. This justifies why the effect of large displacements have long been disregarded in most mechanical models (Blaise et al. 1992; Castera and Morlier 1991; Fourcaud and Lac 1996; Fournier et al. 1994). However, in the case of a vertical stem loaded vertically, the SDA remains problematic because the bending moment is extremely sensitive to small changes in the form of the trunk. The SDA has been discarded in recent mechanical models (Ancelin et al. 1999; Jirasek et al. 2000). In contrast, creep probably goes on, so that this error would tend to increase with the age of the structure. To our knowledge, no mechanical model of tree development takes these viscoelastic effects into account.

Previous works show that the form of a stem is sensitive to the amount of radial growth in the first years of its development (Fournier et al. 1994). Moreover, the dynamics of diameter growth and of loading suggest a considerable impact of the relative kinetics of the two phenomena on the bending of the fruit tree stems, and therefore the unsuitability of an annual time step for their modelling. Indeed, during the first years of growth, axillary loads lead to large bending while the relative increase in I is considerable. The order of occurrence of these growth events is crucial to predict stem bending in a satisfactory way. In an apricot tree, the fact that the weight increase precedes diameter growth is the cause of the large degree of bending observed. The presence of fruit is a major cause of this bending, but it is not the only one. The weight of the leaves and branches is responsible for >50% of the load, suggesting that these results could be extended to the stems of non-fruit species, in particular when they are slender and hold abundant axillaries.

The growth of a branch interacts with the form and orientation of its stems (Cannell and Dewar 1994; Fisher and Stevenson 1981; Wilson 2000). The objective of the mechanical modelling in this context is to explore the consequences of growth on the form of these stems. Reciprocally, the form and orientation of a stem influence its mode of growth through the phenomenon called gravimorphism (Smith and Wareing 1964; Wareing and Nasr 1961). The joined integration of both phenomena in growth models remains currently the object of several works (Alteyrac et al. 1999; Jirasek et al. 2000). In these models, the relation between form and growth are expressed by temporal relations: the deformation during a given period is calculated from the growth of the previous period, and partly controls the growth of the following period. In this context, we believe that the deformations undergone by a stem in early years of growth can be fundamental for the understanding of its long-term development. Indeed, these large displacements are subsequently fixed by the radial growth of the stem. The straightening mechanisms of the stem depend themselves on the growth processes. Even a small difference in stem form at early stages could lead, through the reciprocal dependencies between form and growth, to an important divergence in its later development.

Acknowledgement The authors gratefully thank Jean-Claude Salles (Laboratory of Fruit Arboriculture, INRA Montpellier) for his help with growth and digitalization measurements.

References

Adam B, Sinoquet H, Godin C, Dones N (2000) 3A Version 1.0: un logiciel pour l'acquisition de l'architecture des arbres intégrant la saisie simultanée de la topologie au format AMAPmod et de la géométrie par digitalisation 3D. Guide de l'utilisateur. INRA-PIAF, Clermont-Ferrand

Alméras T (2001) Acquisition de la forme chez des axes ligneux d'un an de trois variétés d'abricotier: confrontation de données expérimentales à un modèle biomécanique. PhD thesis. Agro-Montpellier, Montpellier

Alteyrac J, Fourcaud T, Castera P, Stokes A (1999) Analysis and simulation of stem righting movements in Maritime pine (*Pinus pinaster* Ait.). In: Nepveu G (ed) Proceedings of the IUFRO Working Party F5.01–04, Connection between Silviculture and Wood Quality through Modelling Approaches and Simulation Software, Third Workshop of the IUFRO, 5–12 September 1999, La Londe-Les-Maures, France. INRA-Nancy, Nancy, pp 105–112

Ancelin P, Fourcaud T, Lac P (1999) Non linear structural analysis to investigate tree biomechanics. In: Nepveu G (ed) Proceedings of the IUFRO Working Party F5.01–04, Connection between Silviculture and Wood Quality through Modelling Approaches and Simulation Software, Third Workshop of the IUFRO, 5–12 September 1999, La Londe-Les-Maures, France. INRA-Nancy, Nancy, pp 95–104

Archer R (1986) Growth stresses and strains in trees. In: Timell E (ed) Springer series in wood science. Springer, Berlin Heidelberg New York

Blaise F, Gril J, Fournier M (1992) Introduction de concepts mécaniques dans un logiciel de simulation de la croissance des plantes. In: Thibaud B (ed) Architecture structure et mécanique de l'arbre. LMGC, Montpellier, pp 171–185

Cannell MGR, Dewar RC (1994) Carbon allocation in trees: a review of concepts in modelling. Adv Ecol Res 25:59–104

Castera P, Morlier V (1991) Growth patterns and bending mechanics of branches. Trees 5:232–238

Costes E (1993) The aerial architecture of untrained apricot trees. Acta Bot Gall 140:249–261

Costes E, Audubert A, Jaffuel S, Jay M, Demene M, Lichou J (1995) Chronologie du développement du fruit en relation avec la croissance végétative chez l'abricotier *Prunus armeniaca* L. cv. Rouge du Roussillon. Can J Bot 73:1548–1556

Costes E, Fournier D, Salles J (2000) Changes in primary and secondary growth as influenced by crop load effects in Fantasme apricot trees. J Hortic Sci Biotechnol 75:510–519

Craig J (1989) Introduction to robotics. Addison-Westley, Reading

Fisher J, Stevenson J (1981) Occurrence of reaction wood in branches of dicotyledons and its role in tree architecture. Bot Gaz 142:82–95

Fourcaud T, Lac P (1996) Mechanical analysis of the form and internal stresses of a growing tree by the finite element method. In: Engin AE (ed) Proceedings of the Congress on Engineering Systems Design and Analysis, 1–4 July 1996, ASME, Montpellier. ESDA, New York, pp 213–220

Fournier M, Chanson B, Guitard D, Thibaut B (1991a) Mechanics of standing trees: modelling a growing structure subjected to continuous and fluctuating loads. 1. Analysis of support stresses. Ann Sci For 48:513–525

Fournier M, Chanson B, Thibaut B, Guitard D (1991b) Mechanics of standing trees: modelling a growing structure subjected to continuous and fluctuating loads. 2. Three-dimensional analysis of maturation stresses in a standard broadleaved tree. Ann Sci For 48:527–546

Fournier M, Baillères H, Chanson B (1994) Tree biomechanics: growth, cumulative prestresses, and reorientations. In: Vincent JFV, Srinivasan (eds) Biomimetics. Plenum Press, New York, pp 229–252

Gril J, Fournier M (1993) Contraintes d'élaboration du bois dans l'arbre: un modèle multicouche viscoélastique. In: Actes du 11ème Congrès de Mécanique, July 1993, Lille Villeneuve d'Ascq, France. AUM, Lille Villeneuve d'Ascq, France, pp 165–168

Jirasek C, Prusinkiewicz P, Moulia B (2000) Integrating biomechanics into developmental models expressed using L-systems. In: Spatz HC, Speck T (eds) Plant biomechanics. Thieme, Stuttgart, pp 615–624

KollMann F, Côté W (1968) Principles of wood science and technology. I Solid wood. Springer, Berlin Heidelberg New York

Kozlowski T (1971) Growth and developement of trees, vol II. Cambial growth, root growth, and reproductive growth. Academic Press, New York

Lakhoua H, Crabbe J (1975) Arching and gravimorphism in apples. I. Effects of various degrees of arching on the shape of branching and vigour. Bull Rech Agron Gembloux 10:43–54

Lauri PE, Térouanne E, Lespinasse JM (1997) Relationship between the early development of apple fruiting branches and the regularity of bearing – an approach to the strategies of various cultivars. J Hortic Sci 72:519–530

Leiser AT, Kemper JD (1973) Analysis of stress distribution in the sapling tree trunk. J Am Soc Hortic Sci 98:164–170

Lemaitre J, Chaboche JL (1985) Mécanique des matériaux solides. Bordas, Paris

Lichou J, Audubert A (1989) L'abricotier. CTIFL, Paris

Lichou J, Jay M, Combes J (1997) Variation de la qualité des abricots dans l'arbre. Inf CTIFL 135:30–33

Milne R, Blackburn P (1989) The elasticity and vertical distribution of stress within stems of *Picea sitchensis*. Tree Physiol 5:195–205

Morgan J, Cannell MGR (1987) Structural analysis of tree trunks and branches: tapered cantilever beams subject to large deflections under complex loading. Tree Physiol 3:365–374

Moulia B (1993) Etude mécanique du port foliaire du mais. PhD thesis. Université Bordeaux I, Bordeaux

Polhemus (1993) 3SPACE FASTRAK user's manual. Polhemus, Cochester, VT

Seber GAF (1984) Multivariate observations. Wiley, New York

Smith H, Wareing PF (1964) Gravimorphism in trees. 2. The effect of gravity on bud-break in osier willow. Ann Bot 28:283–295

Thomas R (2000) Analyse des formes de tronc par photogrammetrie pour caractériser la qualité des bois. PhD thesis. ENGREF, Montpellier

Timell T (1986) Compression wood in gymnosperms. Springer, Berlin Heidelberg New York

Timoshenko S (1953) Résistance des matériaux. Première partie: théorie élémentaire et problèmes. Librarie polytechnique C. Béranger, Paris

Timoshenko S (1966) Théorie de la stabilité élastique. Dunod, Paris

Wareing PF, Nasr TAA (1961) Gravimorphism in trees. 1. Effect of gravity on growth and apical dominance in fruit trees. Ann Bot 25:321–340

West PW, Jackett DR, Sykes SJ (1989) Stresses in, and the shape of, tree stems in forest monoculture. J Theor Biol 140:327–343

Wilson BF (2000) Apical control of branch growth and angle in woody plants. Am J Bot 87:601–607